

ELECTRONIC SUPPLEMENTARY INFORMATION FOR

Development of a Simultaneous Electrorotation Device with Microwells for Monitoring the
Rotation Rates of Multiple Single Cells upon Chemical Stimulation

Authors; Masato Suzuki, Shikiho Kawai, Chean Fei Shee, Ryoga Yamada, Seiichi Uchida
and Tomoyuki Yasukawa.

Table of Contents

Appendix: Calculation methods for $-\text{Im}[\text{CM}]$

Figure S1:

Schematic of the fabrication process of the microwell array electrode device.

Figure S2:

Procedure for evaluating the ROT rate of a target cell. (A) Microscopic image of the microwell array electrode device containing the cells. The target cell was selected with a rectangular shape and orange color. (B1) Magnified image of the cell selected in (A). (B2) Cell area defined by Otsu's thresholding was filled with the red color.

Figure S3:

Calculation results of the real or minus imaginary part of the Clausius–Mossotti factor at various frequencies. The parameters for this calculation are, as follows: Cell membrane capacitance (C_m) and cytoplasm conductivity (σ_c) were 9.82 mF m^{-2} and 0.25 S m^{-1} ,

respectively. The cell radius (r) was $6.02\text{ }\mu\text{m}$. The conductivity (σ_e) and relative permittivity ϵ_e of the extracellular solution (the ROT solution) were 74 mS m^{-1} and 78, respectively. The cytoplasm relative permittivity ϵ_c was 103.9.

Figure S4:

Time dependence of distributions of the calculated electric field strength in the microwell when sine waves with $\pi/2$ differences in the phase were applied to microelectrodes a, b, c, and d, respectively. (A) Images of the X-Y plane $15.7\text{ }\mu\text{m}$ above the bottom of the microwell, and sectional planes through the (B) line i – ii and (C) line iii – iv in A. Images were obtained at $t=0$, $T/8$, $T/4$, $3T/8$, and $T/2$, respectively. Red arrows in A represent the vectors of the electric field.

Figure S5:

z-profiles of the field strengths above the center of the microwell.

Figure S6:

Ratio of the number of K562 cells trapped in single microwell at various incubation times.

Figure S7:

Sequential images of a single Jurkat cell rotating in the dashed white circle (ii) in Fig. 3A.

Figure S8:

Trajectory of the x-axis of a characteristic point on the surface of the single cell depicted in Fig. 2B.

Figure S9:

Plot of rotation rates for Jurkat cells to the square of applied voltage.

Figure S10:

(A) Microscopic image extracted from Movie S3. Five randomly selected cells were surrounded by rectangles with various colors. (B) Time-series of the ROT rate of the five cells. One microliter droplet of the ROT solution with ionomycin was added at $t = 10$ s.

Figure S11:

Time-series of the normalized cell radius. One microliter droplet of the ROT solution without (white circle) or with (black circle) ionomycin added at $t = 10$ s.

Figure S12:

Calculated values of $-\text{Im}[\text{CM}]$ at 300 kHz for the various (A) membrane capacitances and (B) membrane conductance. In Fig. S12A, the value of $-\text{Im}[\text{CM}]$ at 9.82 mF m^{-2} in the membrane capacitance, which was the initial state of the Jurkat cell before the addition of ionomycin, was filled in black.

Supporting Movies

Movie S1:

Movie of the rotating cell that was selected through the process shown in Fig. S2.

Movie S2:

Simultaneous ROT of the Jurkat cells by the microwell array electrode device at an AC voltage of 300 kHz and 2 Vpp.

Movie S3:

Simultaneous ROT of the Jurkat cells by the microwell array electrode device at an AC voltage of 300 kHz and 2 Vpp. The ionomycin-containing solution was added 10 s after the video commenced.

Movie S4:

Movie of the rotating cell indicated as (i) in Fig. S5 or Movie S3.

Movie S5:

Simultaneous ROT of the Jurkat cells by the microwell array electrode device at an AC voltage of 300 kHz and 2 Vpp. The solution without ionomycin was added 10s after the video commenced.

Appendix: Calculation methods for -Im[CM]

CM factor of the equivalent homogeneous particle in a single-shell model is given by:

$$CM = \frac{\underline{\varepsilon}_2' - \underline{\varepsilon}_1}{\underline{\varepsilon}_2' + 2\underline{\varepsilon}_1}$$

where $\underline{\varepsilon}_2'$ is the complex permittivity of equivalent homogeneous particle and $\underline{\varepsilon}_1$ is the complex permittivity of the solution. The complex permittivity of the solution is given by:

$$\underline{\varepsilon}_1 = \varepsilon_1 + \frac{\sigma_1}{j\omega}$$

where ε_1 and σ_1 are the permittivity and the conductivity of the solution, respectively, ω is the angular frequency, and j is the imaginary unit. The complex permittivity of the cell in the single-shell model is given by:

$$\underline{\varepsilon}_2' = \frac{\underline{c}_m R \underline{\varepsilon}_2}{\underline{c}_m R + \underline{\varepsilon}_2}$$

where \underline{c}_m is the complex capacitance of the membrane, $\underline{\varepsilon}_2$ is the complex permittivity of cytoplasm, and R is cell radius. The complex capacitance of the membrane and the complex permittivity of cytoplasm is given by:

$$\underline{c}_m = c_m + \frac{g_m}{j\omega}$$

$$\underline{\varepsilon}_2 = \varepsilon_2 + \frac{\sigma_2}{j\omega}$$

where c_m is the membrane capacitance per unit area, g_m is the membrane conductance per unit area, and ε_2 and σ_2 are the permittivity and conductivity of the cytoplasm, respectively.

We calculated the imaginary part of CM by using the above equations by employing the

following parameters: $\epsilon_1 = 78 \epsilon_0 \text{ F m}^{-1}$, $\sigma_1 = 0.074 \text{ S m}^{-1}$, $\epsilon_2 = 87 \epsilon_0 \text{ F m}^{-1}$, $\sigma_2 = 0.25 \text{ S m}^{-1}$, $c_m = 9.82 \text{ mF m}^{-2}$, and $R = 6.02 \text{ }\mu\text{m}$. We employed zero and 60 nS as the membrane conductance before and after adding ionomycin, respectively. The values of g_m were calculated by dividing membrane conductance by the cell surface area ($4\pi R^2$).

Figure S1. Schematic of the fabrication process of microwell array electrode devices.

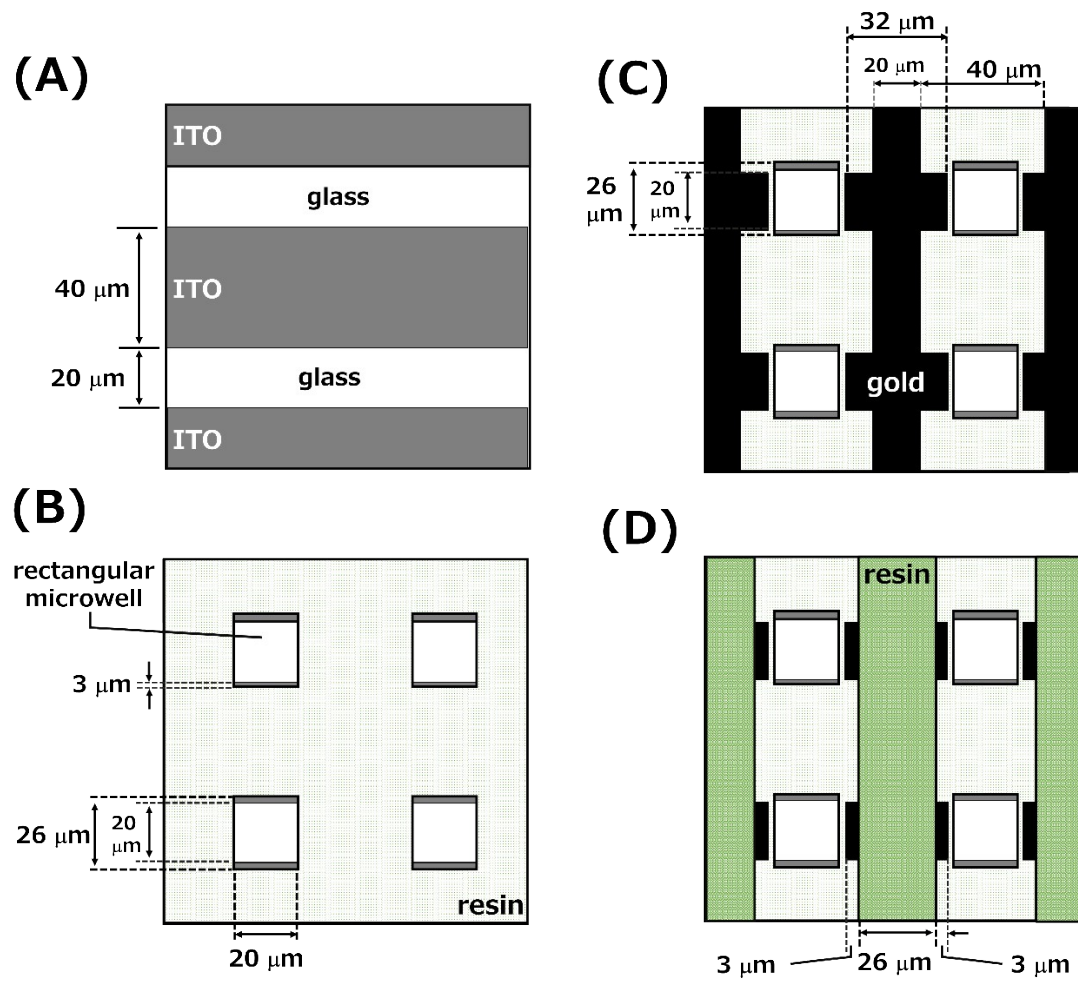


Figure S2. Procedure for evaluating the ROT rate of a target cell. (A) Microscopic image of the microwell array electrode device containing the cells. The target cell was selected with a rectangular shape and orange color. (B1) Magnified image of the cell selected in (A). (B2) Cell area defined by Otsu's thresholding was filled with the red color.

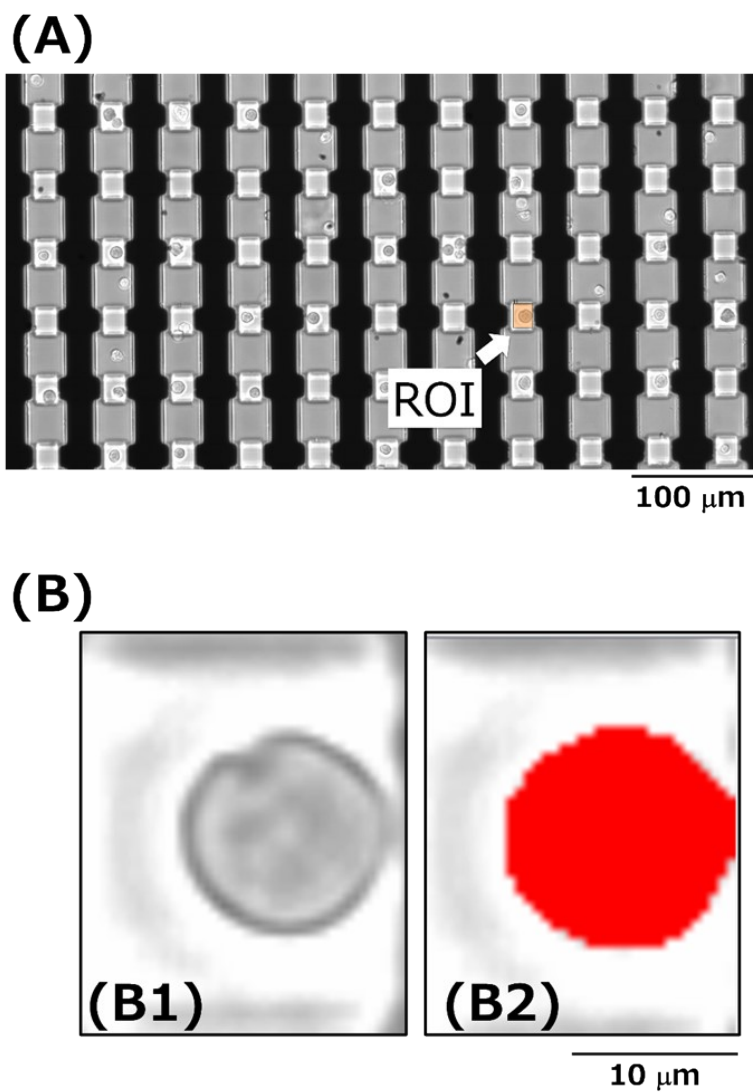


Figure S3. Calculation results of the real or minus imaginary part of the Clausius–Mossotti factor at various frequencies. The parameters for this calculation are, as follows: Cell membrane capacitance (C_m) and cytoplasm conductivity (σ_c) were 9.82 mF m^{-2} and 0.25 S m^{-1} , respectively. The cell radius (r) was $6.02 \text{ }\mu\text{m}$. The conductivity (σ_e) and relative permittivity ϵ_e of the extracellular solution (the ROT solution) were 74 mS m^{-1} and 78, respectively. The cytoplasm relative permittivity ϵ_c was 103.9.

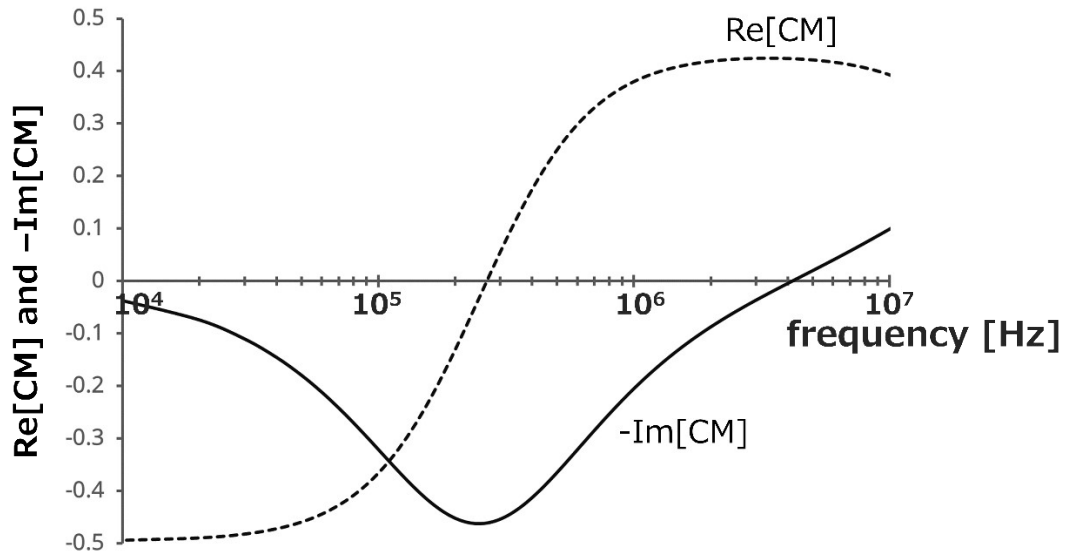


Figure S4. The distribution of the calculated electric field strength in the microwell when sine waves with $\pi/2$ differences in a phase were applied to microelectrodes a, b, c, and d, respectively. (A) An X-Y plane 15.7 mm above the bottom of the microwell, sectional planes through the (B) line i – ii and (C) line iii – iv in A. Red arrows in Fig. S4A represent the vectors of the electric field.

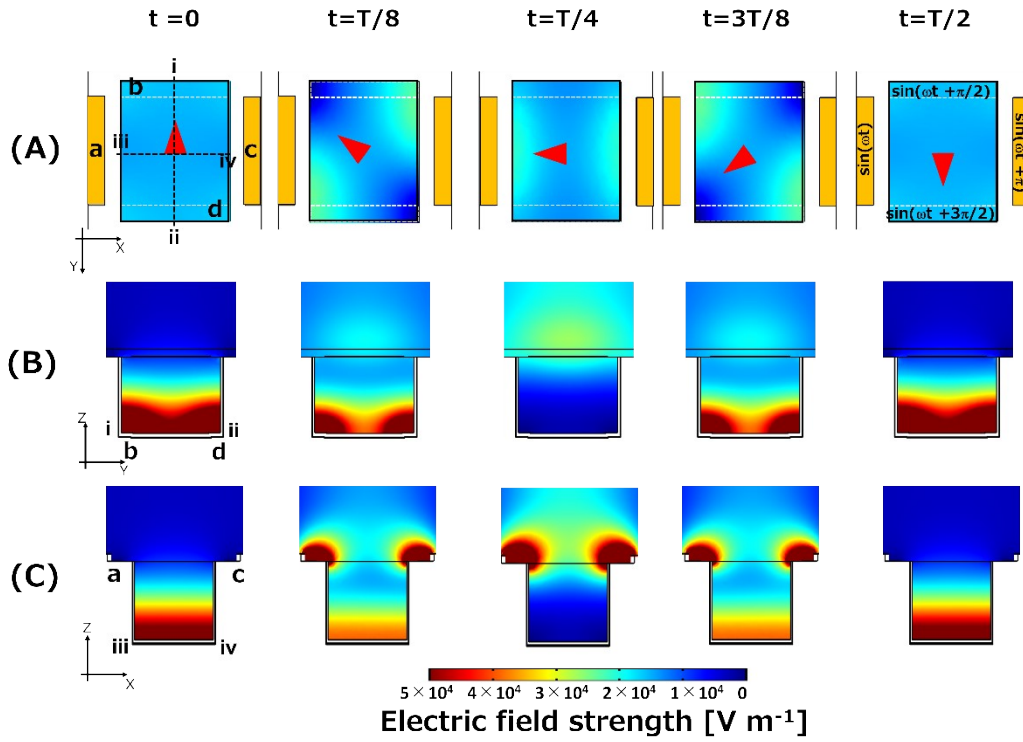


Figure S5. Plot of the electric field strength from the center of the bottom of the microwell to outside of the microwell.

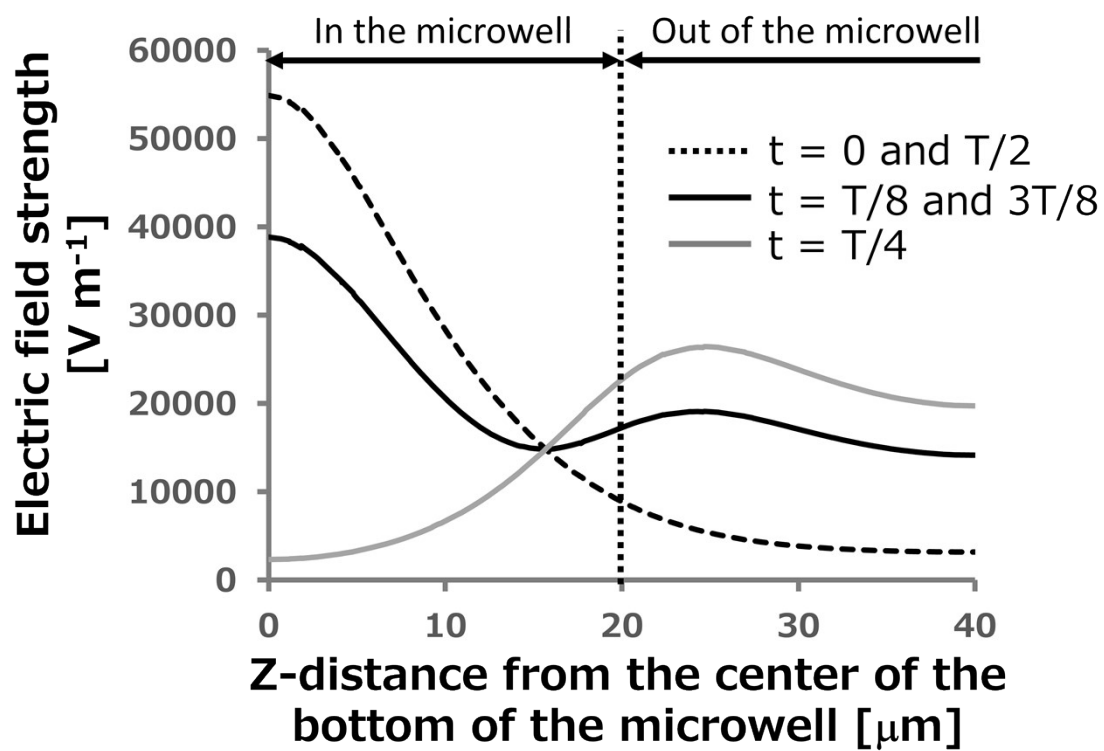


Figure S6. Ratio of the number of K562 cells trapped in single microwell at various incubation time.

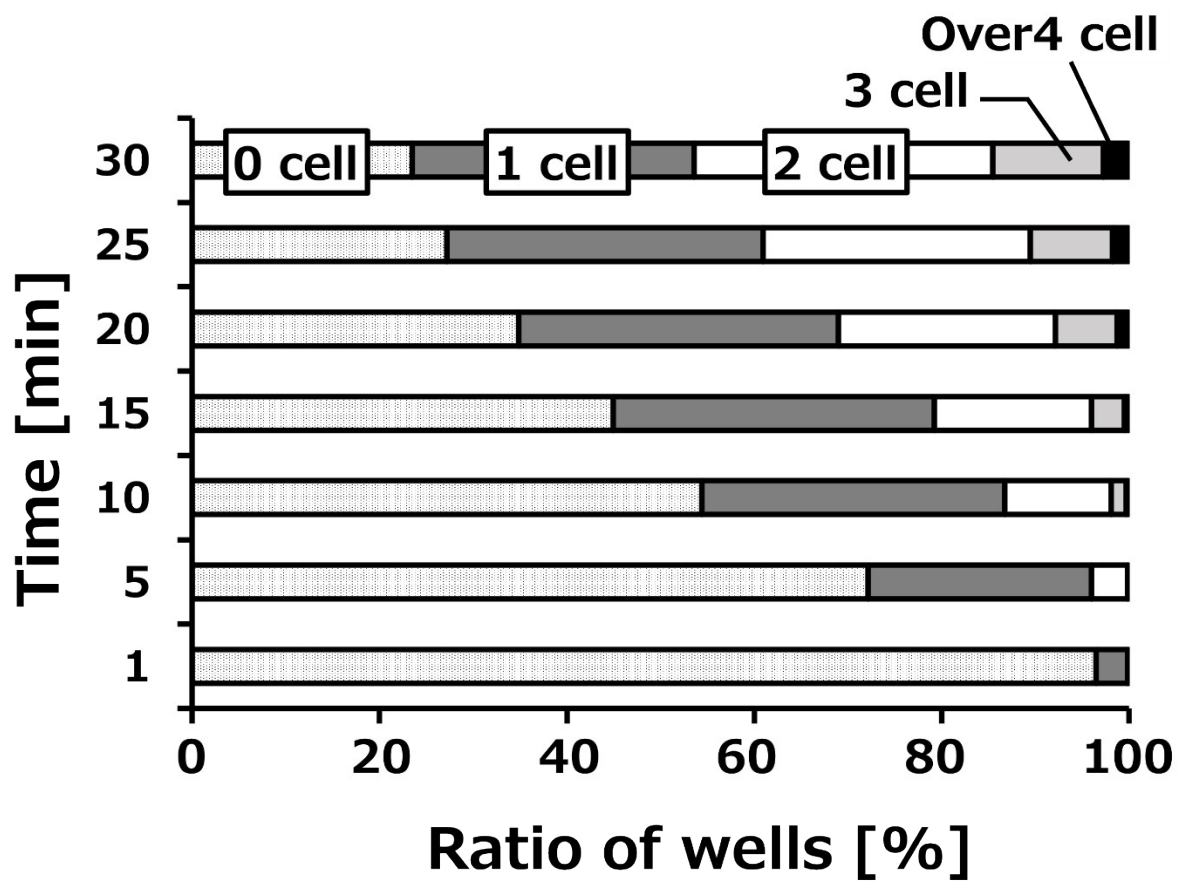


Figure S7. Sequential images of a single Jurkat cell rotating in the dashed white circle (ii) in Fig. 3A.

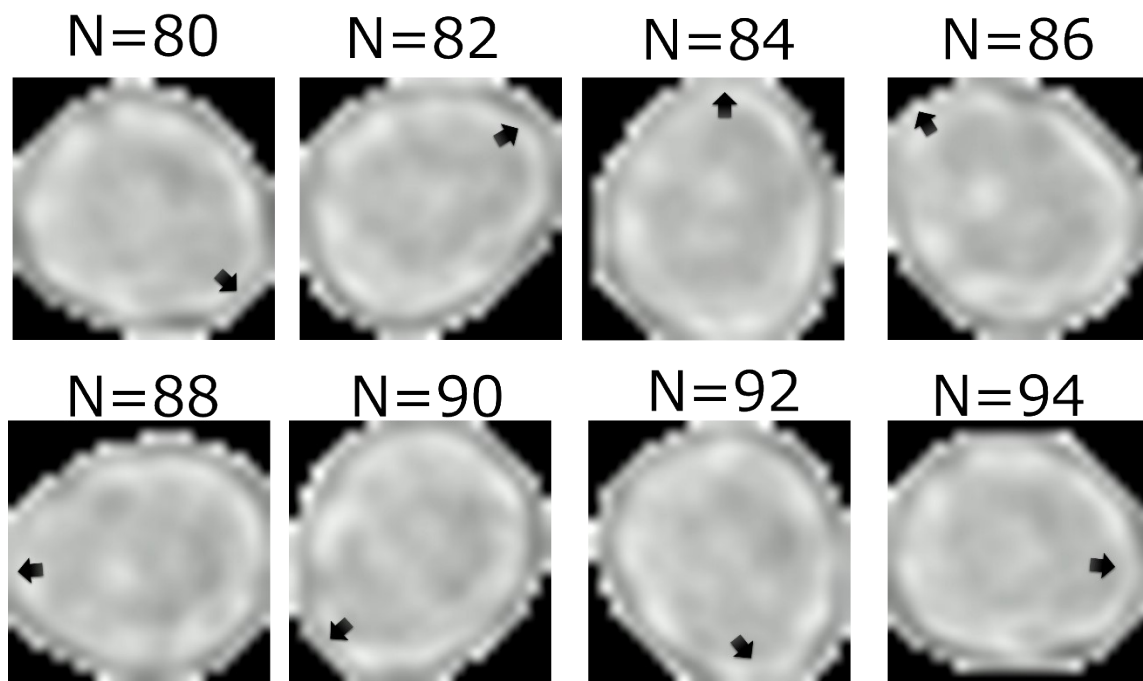


Figure S8. Trajectory of the x-axis of a characteristic point on the surface of the single-cell depicted in Fig. 2B.

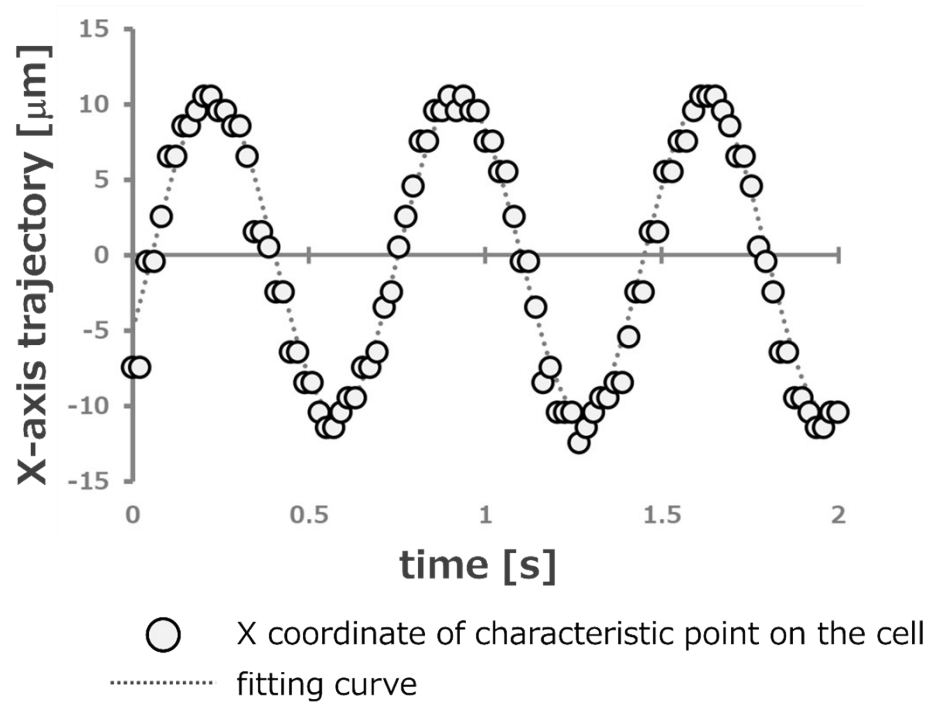


Figure S9. Plot of rotation rates for Jurkat cells to square of applied voltage.

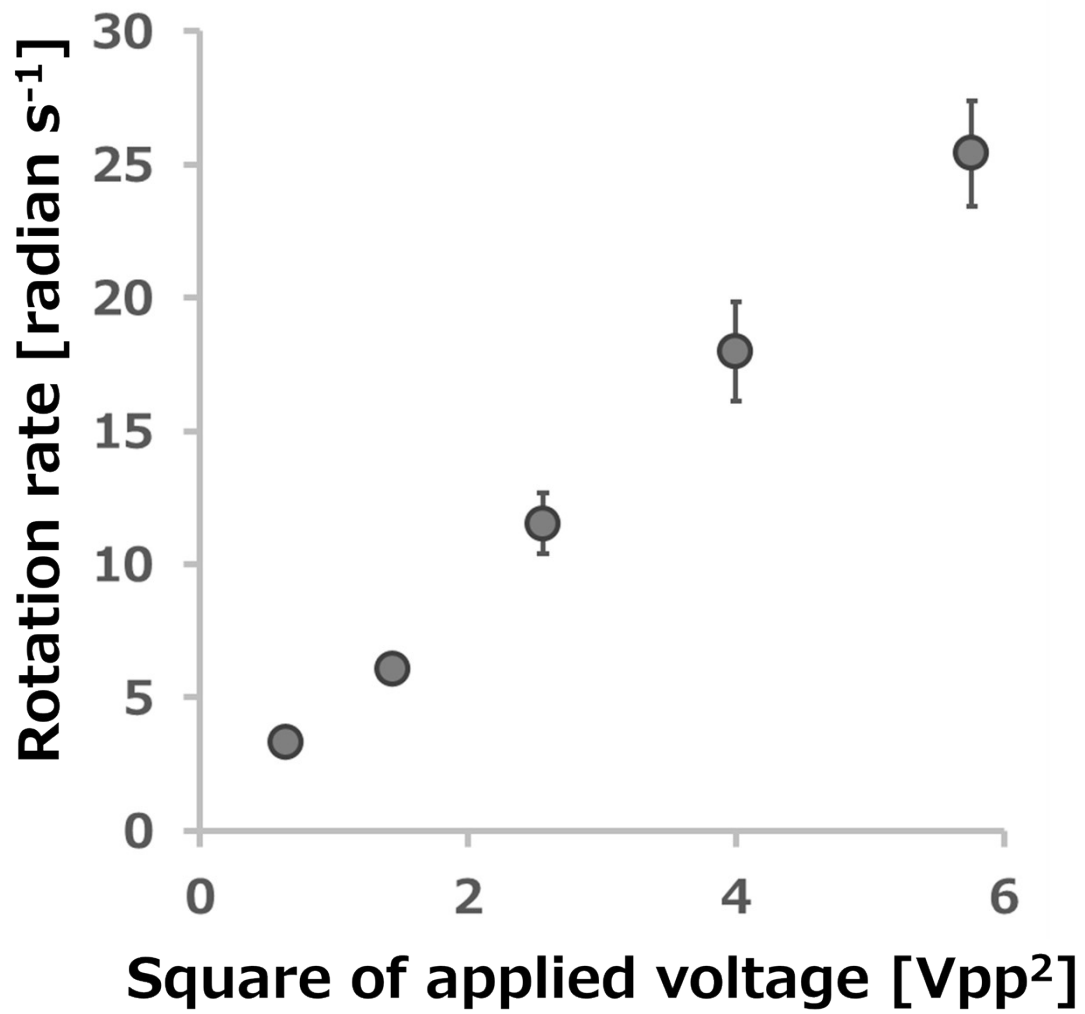


Figure S10. (A) Microscopic image extracted from Movie S3. Five randomly selected cells were surrounded by rectangles with various colors. (B) Time-series of the ROT rate of the five cells. One microliter droplet of the ROT solution with ionomycin was added at $t = 10$ s.

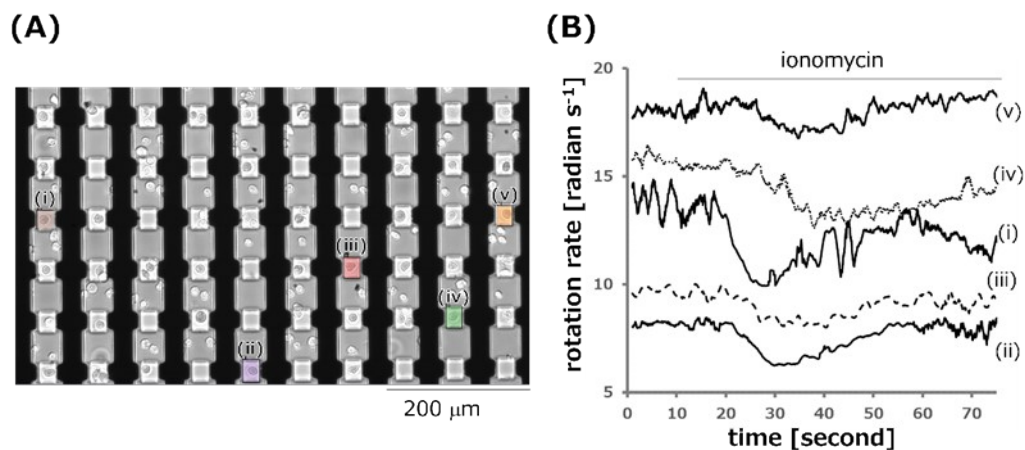


Figure S11.

Time-series of the normalized cell radius. One microliter droplet of the ROT solution without (white circle) or with (black circle) ionomycin added at $t = 10$ s.

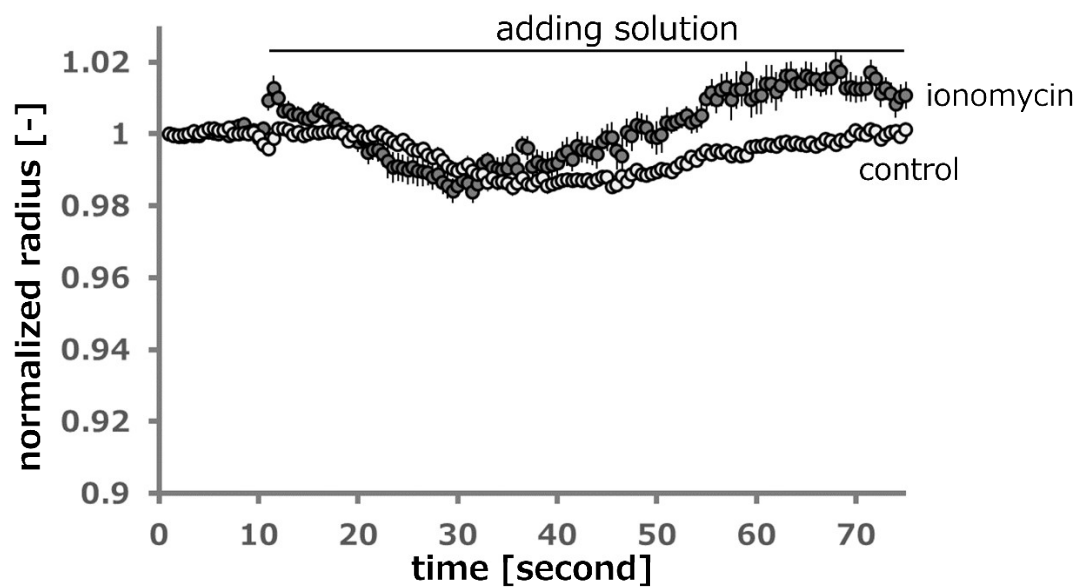


Figure S12. Calculated values of $-\text{Im}[\text{CM}]$ at 300 kHz for the various (A) membrane capacitances and (B) membrane conductance. In Fig.S12A, the value of $-\text{Im}[\text{CM}]$ at 9.82 mF m^{-2} in the membrane capacitance, which was the initial state of the Jurkat cell before the addition of ionomycin, was filled in black.

